International Journal for Modern Trends in Science and Technology
Volume 10, Issue 11, pages 48-59.
ISSN: 2455-3778 online
Available online at: http://www.ijmtst.com/vol10issue11.html
DOI: https://doi.org/10.46501/IJMTST1011006

Integration of ANN Controller for AGC in Hydro-Thermal Systems with Dynamic Turbine Time Constants and Variable Power System Loading Conditions

Dr. J. Srinu Naik | P.V.Guru Susmanth | D.Harish Kumar | A.Babu Reddy | A.Jayavardhan

Department of Electrical and Electronics Engineering, Chadalawada Ramanamma Engineering College, Andhra Pradesh, India.

To Cite this Article
Dr. J. Srinu Naik, P.V.Guru Susmanth, D.Harish Kumar, A.Babu Reddy and A.Jayavardhan, Integration of ANN Controller for AGC in Hydro-Thermal Systems with Dynamic Turbine Time Constants and Variable Power System Loading Conditions, International Journal for Modern Trends in Science and Technology, 2024, 10(11), pages. 48-59. https://doi.org/10.46501/IJMTST1011006

Article Info
Received: 29 October 2024; Accepted: 22 November 2024.; Published: 25 November 2024.

ABSTRACT

The integration of an Artificial Neural Network (ANN) controller for Automatic Generation Control (AGC) in hydro-thermal power systems presents a novel approach to managing the dynamic and complex nature of modern power grids. This study focuses on enhancing AGC performance by addressing the challenges posed by dynamic turbine time constants and variable power system loading conditions. Traditional AGC methods often fall short in handling these complexities due to their limited adaptability. In contrast, ANN controllers, with their ability to learn and adapt to changing system dynamics, offer a robust solution. The ANN controller is designed to continuously adjust control parameters in real-time, ensuring optimal frequency regulation and stability across varying load conditions. Using MATLAB/SIMULINK, the hydro-thermal system is simulated to evaluate the performance of the ANN controller under different scenarios. The results demonstrate significant improvements in system stability, response time, and frequency regulation compared to conventional control methods. This research highlights the potential of ANN controllers to enhance the reliability and efficiency of AGC in hydro-thermal systems, paving the way for more resilient and adaptive power system management.

***KEYWORDS:** Automatic Generation Control (AGC), Hydro-Thermal Power Systems, Artificial Neural Network (ANN) Controller, Load Frequency Control (LFC), Power System Stability*

1.INTRODUCTION

The power system frequency, voltage profile, and tie-line flows are critical parameters that must be strictly maintained at their nominal values. Voltage is regulated by nullifying the reactive power mismatch between generation and demand using automatic voltage regulators (AVR) [1]. In contrast, frequency and prescheduled interchanges are maintained using Automatic Generation Control (AGC) [2]. The practical operation of AGC and the role of various plant control equipment in AGC operations have been well documented [3-4]. Initial AGC studies focused independently on thermal and hydro power systems [5-6]. Key aspects of tie-line bias control, such as the effect of load variation on area governing characteristics and tie-line bias settings, were also explored [7]. Classical control theory has been utilized to optimize the controller gains and bias factors in the transfer function modeling of two-area non-reheat thermal power systems [8]. Optimal control theory has also been employed to develop full state feedback controllers for "Megawatt Frequency Control" problems [9-10]. However, because all power system model states are not accessible, suboptimal AGC controllers have been designed using only the practically available states at control centers [11]. Studies extended to multi-area power systems with reheat turbines have also incorporated the effects of speed governor dead bands and power generation constraints [12]. AGC operations are managed by control centers located far from the actual generating units, transmitting control signals as discrete control pulses at regular intervals [13]. This discrete control operation minimizes turbine wear and tear and reduces excessive movement of governor control valves. It also reduces the burden on data sampling equipment by sampling frequency and tie-line power deviations at regular intervals. Due to these benefits, research shifted to discrete AGC analysis of multi-area power systems [14–17]. The dynamic performance of AGC systems largely depends on the optimal selection of controller gains. Various intelligent adaptive controls have been developed for optimal AGC operations, evaluated using performance indices such as Integral Squared Error (ISE), Integral Absolute Error (IAE), Integral Time Multiplied Absolute Error (ITAE), and Integral Time Multiplied Squared Error (ITSE) [18–25]. Comparative studies revealed that the ISE criterion offers the best dynamic performance under all operating conditions [26]. Consequently, this study uses the ISE criterion to optimize controller gains. Over recent decades, the increased penetration of hydro power in existing networks has spurred research interest. Studies on isolated hydro power systems have evaluated AGC system dynamics, developing mechanical and electric hydraulic speed governor models [27]. Optimal settings for mechanical hydraulic speed governors, including temporary droop and dashpot time constants, and electric speed governor gain coefficients, were recommended based on practical and theoretical analyses [28–30]. Linearized hydro turbine models have also been developed and validated with actual field tests [31]. This study uses these linearized models to investigate hydro-thermal power systems under variable loading conditions. Power system loads vary significantly throughout the day, necessitating hour-ahead or day-ahead generation schedules. Hydro-thermal power systems operate under different loading conditions based on these schedules. Literature indicates that AGC model parameters such as frequency bias factor (Bi), power system inertia gain (Kp), and power system time constant (Tp) vary with plant loading [32–35]. Additionally, steam and hydro turbine time constants also change with power system loading conditions. Despite numerous AGC studies on hydro-thermal power systems, no study has yet considered the variations of both steam and hydro turbine time constants with loading conditions. This study addresses this gap by evaluating the dynamic performance of hydro-thermal power systems under partial load operations, considering the variations in turbine time constants. Empirical formula-based hydro electric governor settings recommended by IEEE are found inadequate for hydro-thermal systems. For the first time, hydro governor settings are optimized using meta-heuristic techniques, simultaneously with controller gains for various loading conditions. Comparing dynamic responses with conventional and optimized hydro governor settings reveals that the optimization-based settings significantly improve performance across all loading conditions. This paper also discusses the optimal selection of sampling periods for discrete AGC operations in hydro-thermal systems. By integrating an Artificial Neural Network (ANN)

controller, this study aims to enhance AGC performance in hydro-thermal systems with dynamic turbine time constants and variable loading conditions as shown in figure 1. ANN controllers, with their adaptive learning capabilities, offer a robust solution to manage the non-linearities and uncertainties in such complex systems, providing improved stability, response time, and frequency regulation compared to traditional methods [38-39]. The ANN controller is designed to continuously adjust control parameters in real-time, ensuring optimal frequency regulation and system stability across varying load conditions. Using MATLAB/SIMULINK, the hydro-thermal system is simulated to evaluate the performance of the ANN controller under different scenarios [40-42]. The results demonstrate significant improvements in system stability, response time, and frequency regulation compared to conventional control methods. This research highlights the potential of ANN controllers to enhance the reliability and efficiency of AGC in hydro-thermal systems, paving the way for more resilient and adaptive power system management.

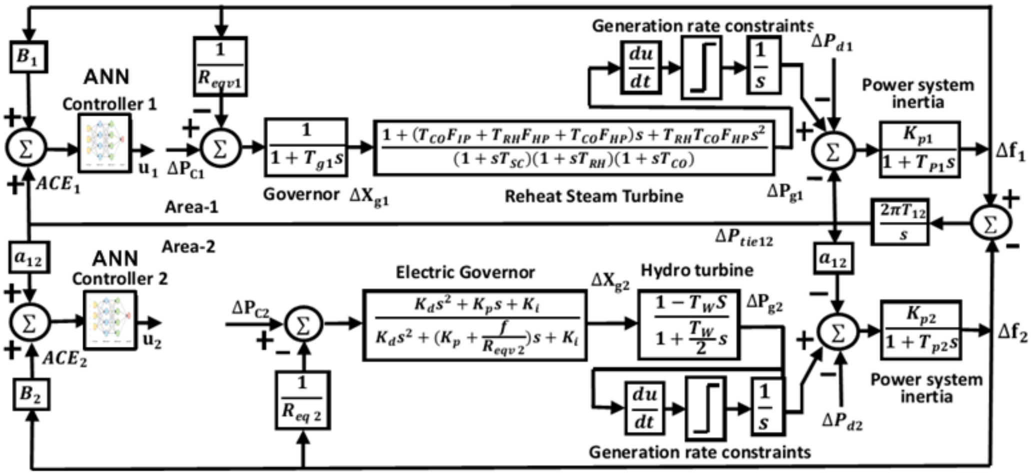

Fig. 1.proposed ANN control based AGC model of two area hydro-thermal power system

II. Methodology to Calculate Steam and Hydro Turbine Time Constants

The mathematical approaches for determining the steam and hydro turbine time constants from plant data under various loading scenarios have been described.

A. Steam turbine time constant calculations

Figure 2 shows a steam vessel with input and output ports, which may be used to depict the steam chest, repeater, and crossover chambers. Using the mass continuity equation, we can calculate the time constant of the steam vessel, as shown in [37]:

$$\frac{dw}{dt} = V_{ves}\frac{dp}{dt} = Q_{in} - Q_{out} \qquad (1)$$

The variables: W for mass of steam in vessel, V_{ves} for volume of steam vessel, ρ for steam density, Q for mass flow rate, and b for time are all included. The pressure entering the vessel is considered to be directly proportional to the flow leaving it. As a result, it's also codified as:

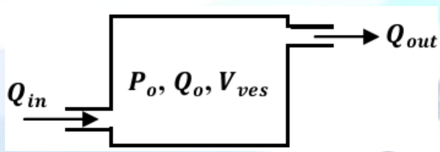

Fig. 2. Steam vessel considered for time constant calculations

$$Q_{out} = \frac{Q_O}{P_O} P \qquad (2)$$

Where, P = Pressure of steam vessel, Po = Rated steam pressure and Qo = Rated flow coming out from the vessel. Let us assume that temperature of vessel is constant. Then, it can be written as:

$$\frac{d\rho}{dt} = \frac{dP}{dt}\frac{\partial\rho}{\partial P}\Big|_{T(o_C)} \qquad (3)$$

The change in steam density w. r. to pressure $\partial\rho/\partial P$ at a given temperature can be obtained from steam tables. From Eqns. (1), (2) and (3), it is obtained:

$$Q_{in} - Q_{out} = V_{ves} \frac{dP}{dt}\frac{\partial\rho}{\partial P}\Big|_{T(oC)} \quad (4)$$

Or, $$Q_{in} - Q_{out} = V_{ves} \frac{\partial\rho}{\partial P}\Big|_{T(oC)} \frac{P_0}{Q_0}\frac{dQ_{out}}{dt} \quad (5)$$

Or, $$Q_{in} - Q_{out} = T_V \frac{dQ_{out}}{dt} \quad (6)$$

Where, $$T_V = \frac{P_0}{Q_0} V_{ves} \times K_{ves} \quad (7)$$

And $$K_{ves} = \frac{\partial\rho}{\partial P}\Big|_{T(oC)} \quad (8)$$

Taking Laplace transform of Eqn. (6), it is found:

$$Q_{in} - Q_{out} = T_v s Q_{out} \quad (9)$$

Or, $$\frac{Q_{out}}{Q_{in}} = \frac{1}{1+T_V s} \quad (10)$$

With the time constant TV, the transfer function of a steam vessel is represented by Eqn. (10). Steam chest, reheater, and cross-over time constants were obtained using Eqns. (7) and (8). In most cases, you can easily get the values of Po, Qo, and $Xaey$. Nevertheless, the most important aspect is to get $Kaey$, which may be determined using basic curve fitting methods.

B. Hydro turbine time constant calculations

Figure 3 depicts the hydro turbine configuration with penstock. Using Newton's second law of motion, the following equation (shown below) has been developed for the water beginning time constant Tw, commonly known as the water acceleration time in penstock:

$$(\rho l_p A_p)\frac{d\Delta v_P}{dt} = -A_p(\rho g)\Delta h_g \quad (11)$$

Where, lp=Length of penstock, vp=Water velocity in

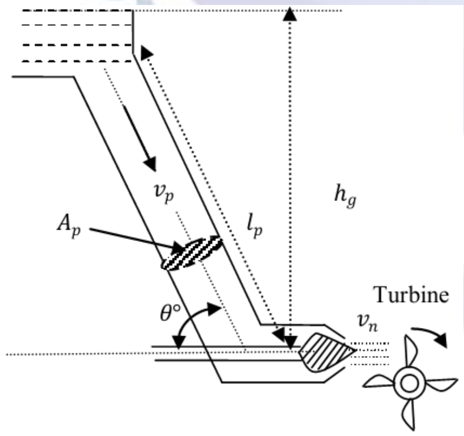

Fig. 3. Hydro turbine setup with penstock

penstock, Ap= Cross-sectional area of penstock, ρ=Water mass density, g=Acceleration constant, $\rho l_p A_p$ =Mass of water in the penstock, $(\rho g)\Delta h_g$ = Incremental change in pressure at turbine gate, t=time.

Dividing Eqn. (11) by $A_p \rho g h_{g0} v_{g0}$ to normalize the acceleration equation, we get:

$$\frac{L_P V_{P0}}{g h_{g0}} \frac{d}{dt}\left(\frac{\Delta v_g}{v_{g0}}\right) = -\frac{\Delta h_g}{h_{g0}} \quad (12)$$

Or, $$Tw \frac{d\Delta \bar{v}_g}{dt} = -\Delta \bar{h}_g \quad (13)$$

Where, according to definition:

$$T_w = \frac{l_P v_{P0}}{g h_{g0}} \quad (14)$$

The normalised values are denoted by the super bar "-" and the original operating point is represented by the subscript "o". The product of the pipe's cross-sectional area and the water's velocity, denoted as $q0 = A_P v_{P0}$, represents the mass flow rate. We obtain: by inserting v_{P0} in Eqn. (14).

$$T_w = \frac{l_p q0}{g A_p h_{g0}} \quad (15)$$

To find the water starting time constant of hydro turbines under various loading situations, we employed Eqn. (15).

III. Hydro-Thermal Power System Modeling

The transfer function modeling of thermal as well hydro power systems is as follows:

A. Thermal Power System

Thermal power systems have taken reheat turbines into account. Fig. 4 shows a typical reheat turbine transfer function block diagram. Based on the transfer function block diagram, the following is the equation for the reheat turbine's transfer function:

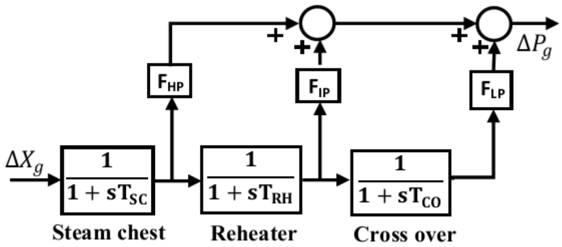

Fig. 4. Transfer function block diagram of reheat turbine

$$G_{RH}(s) = \left\{\left(F_{IP} + \frac{F_{LP}}{(1+sT_{CO})}\right)\frac{1}{(1+sT_{RH})} + F_{HP}\right\}\frac{1}{(1+sT_{SC})} \quad (16)$$

$$G_{RH}(s) = \frac{(F_{HP}+F_{IP}+F_{LP})+(T_{CO}F_{IP}+T_{RH}F_{HP}+T_{CO}F_{HP})s+T_{RH}T_{CO}F_{HP}\, s^2}{(1+sT_{SC})(1+sT_{RH})(1+sT_{CO})} \quad (17)$$

The sum of power fraction factors is equal to 1 p.u.; FHP+FIP+FLP=1. Thus, GRH (s) can be written as:

$$G_{RH}(s) = \frac{1+(T_{CO}F_{IP}+T_{RH}F_{HP}+T_{CO}F_{HP})s+T_{RH}T_{CO}F_{HP}\,s^2}{(1+sT_{SC})(1+sT_{RH})(1+sT_{CO})} \quad (18)$$

The transfer function modelling of thermal systems has made use of Eqn. (18), which captures the dynamics of reheat turbines.

B. Hydro Power System

The dynamic analysis of hydropower systems has taken into account both linear and non-linear models of hydro turbines and speed governors. Here are the models:

1) Linearized hydro turbine and speed governor models

According to references [27, 31], the hydro turbine's approximate linearized model is as follows:

$$G_{HY}(s) = \frac{1-T_W s}{1+\frac{T_\omega}{2}s} \quad (19)$$

The traditional mechanical hydraulic governor was shown to be inferior to the hydro electric governors [27]. Consequently, while modelling hydropower systems, a linearized model of a PID-based hydroelectric speed regulator has been taken into account. Here is the electric governor's transfer function:

$$G_{gov}(s) = \frac{1}{R_{HY}}\left(\frac{k_d s^2+k_P s+k_i}{k_d s^2+(k_p+f/R_{HY})s+k_i}\right) \quad (20)$$

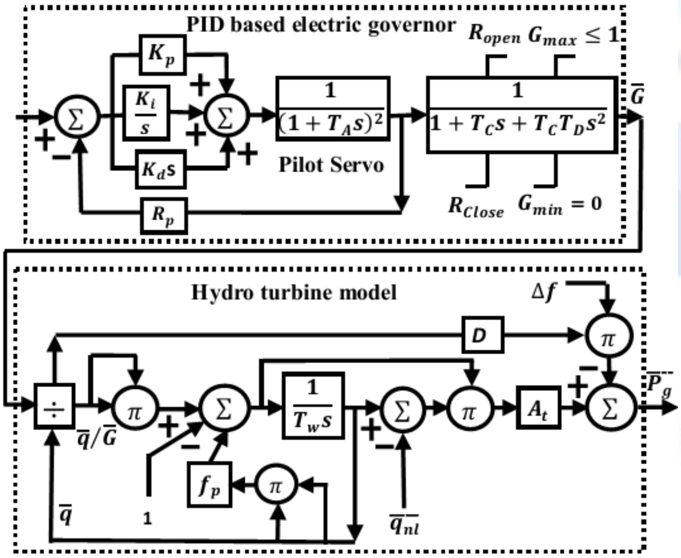

Fig. 5. Non-linear model of hydro turbine in conjunction with PID based hydraulic speed governor.

The speed governor's proportional, integral, and derivative gains are represented by Kp, Ki, and Kd, respectively. The usual empirical formulae suggested by the IEEE working group [30] are usually used to compute these improvements.

2) Non-linearized models of hydro turbines and speed governors

The comprehensive non-linear models are taken into consideration for the study in this part [30]. Fig. 5 depicts the non-linear model of the hydro turbine and PID-based speed governor with a non-elastic water column. The following parameters are used in the non-linear parameters:

q= Flow rate at any operating point ($m3/s$), qr=Rated flow rate ($m3/s$), qnl=Flow rate at no load ($m3/s$), h_r= Rated head of turbine (m), h_f=Head loss due to friction in penstock (m), At=Proportionality constant. The proportionality constant At is calculated based on the ratings of hydro turbine as well as generators using the expression as given below:

$$A_t = \frac{\text{Turbine rating }(P_{tr})}{\text{Generator rating }(P_{gr})\bar{h}_r(\bar{q}_r-\bar{q}_{nl})} \quad (21)$$

TA= Pilot servo time constant(s), TD= Gate servo time constant(s), TC= Gate servo gain, $Ropen$=Rate of valve opening ($p.u./s$), $Rclose$=Rate of valve closing ($p.u./s$), $Gmax$=Max gate opening ($p.u.$), $Gmin$= Min gate opening ($p.u.$). These parameter values of turbine and hydraulic speed governor are given in the Appendix.

C. Equivalent Modeling of Parallely Operated Coherent Generating Units:

The thermal power system has four generating units; each of 500MW capacity and having the total area capacity of 500×4=2000MW. Similarly, hydro power system consists of eight generating units; each of 250MW, thus having the total area capacity of 250×8=2000MW.

It has been considered that the units in their respective areas are coherent. Therefore, the units are represented by a single unit having equivalent inertia constant. Typically, the equivalent inertia of „n" generating units having individual machine ratings of $S1$, $S2$, $S3$…, Sn and inertia constants $H1$, $H2$, $H3$…,Hn is calculated as follows [36]:

$$H_{eqv} = \frac{H_1S_1+H_2S_2+\cdots+H_nS_n}{S_{system}}, S \quad (22)$$

Where, $Ssystem=S1+S2+\cdots+Sn$ (23)

If D is the system damping factor, then power system time constants Tp and gains Kp are calculated as follows:

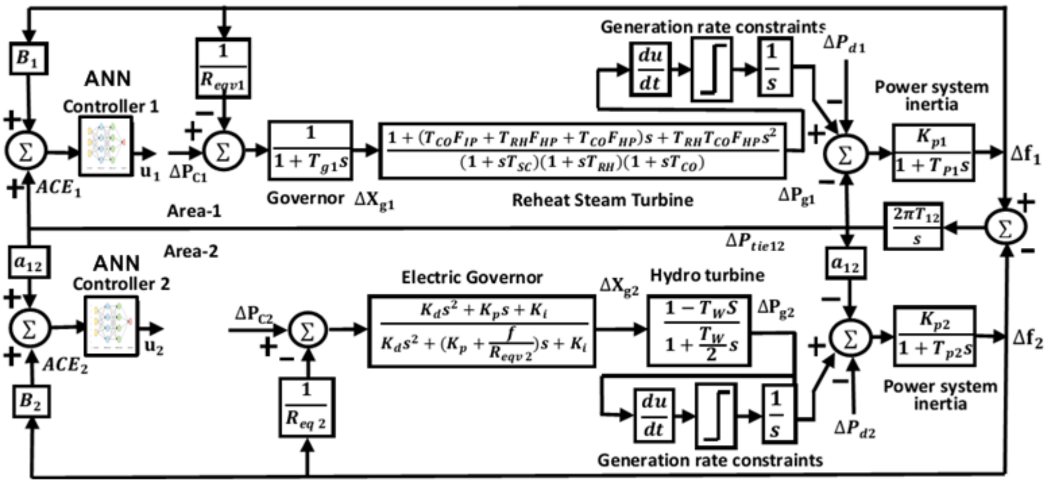

Fig. 6. ANN control based AGC model of two area hydro-thermal power system

$$T_P = \frac{2H_{eqv}}{D\cdot f}s, K_P = \frac{1}{D}Hz\ /\ Mw_{p\cdot u} \quad (24)$$

The combined action of all the producing units' speed governors determines the power system's steady state frequency deviation. If "n" producing units, according to their respective machine ratings, have speed droops of $R1$, $R2$, $R3\ldots$, Rn. After a load disturbance of ΔPd, the steady state frequency deviation may be determined as follows:

$$\Delta f_{ss} = \frac{-\Delta P_d}{(1/R_{eqv})+\mathrm{D}}Hz \quad (25)$$

$$R_{eqv} = \frac{1}{\frac{1}{R_1}\left(\frac{S_1}{S_{system}}\right)+\frac{1}{R_2}\left(\frac{S_2}{S_{system}}\right)+\cdots+\frac{1}{R_n}\left(\frac{S_n}{S_{system}}\right)}Hz\ /\ MW_{p\cdot u} (26)$$

The speed droop characteristics from separate machine rating bases to the common power system base are converted using the multiplying factors $SiSsystem$. The results of the computations indicate that the inertia constant (H) and speed regulation (R) comparable values on a shared system basis match those for a single machine rating.

D. AGC Transfer Function Model of Two Area Hydro-Thermal Power System

Fig. 6 displays the two region hydro-thermal power system's transfer function block diagram. (Thermal system in area 1 and hydro system in area 2). Since the generating units operating inside the areas are coherent, an equivalent single generating unit representing each area has been created, with parameters determined by applying the corresponding equations (22)–(23). The raise and lower operations of power generating units were restricted by the generation rate limits of 3% per minute for thermal units and 270%, 360% per minute for hydro units. To operate the controllers into discrete mode, the zero-order hold circuit is applied to the control signals.

E. Optimization of Controller Gains and Hydro Governor Parameters

The controller gains for both regions are comprised of a total of five variables, or parameters: The hydro governor parameters, referred to as Kp, Ki, and Kd, are to be optimised concurrently with $KI1$, $KI2$, and $K\mathbf{R}$. For the optimisation issue, the ISE performance index criteria has been used. The minimised ISE objective function may be found as follows:

$$J = \Sigma_{k=0}^{\infty}\left\{|\Delta f_i(k)|^2 + \left|\Delta P_{tie\ ij}(k)\right|^2\right\}\Delta T \quad (27)$$

Where, Δf_i , $\Delta P_{tie\ ij}$ are the frequency and tie-line power

Variances and ΔT is the discrete controller's sampling time. For the investigation, a 1.5-second sample duration has been taken into consideration. Because of

its quick convergence properties, the "particle swarm optimisation" (PSO) technique is employed for problem optimisation [19]. But the PSO is just meant to show the outcomes. The method that is being provided may be used with any other meta-heuristic algorithm.

IV. Proposed Neural Network Model:

For a single-input, single-output (SISO) control system, let:

- $x(t)$ be the input at time t,
- $u(t)$ be the control output at time t,
- $y(t)$ be the actual output of the system at time t.

The neural network consists of an input layer, a hidden layer, and an output layer as shown in fig.7. Let:

- *wij* be the weight connecting the i-th node in the input layer to the j-th node in the hidden layer,
- *vj* be the bias of the j-th node in the hidden layer,
- *zj*(t) be the output of the j-th node in the hidden layer.

Similarly, let:

- *bk* be the bias of the k-th node in the output layer,
- *wjk* be the weight connecting the$j$-th node in the hidden layer to the k-th node in the output layer,
- *yk*(t) be the output of the k-th node in the output layer.

a. Forward Pass Equations:

The forward pass of the neural network can be expressed as follows:

Hidden Layer Output (*zj*(t)):

$$z_j(t) = \sigma\left(\Sigma_i w_{ij} \cdot x(t) + v_j\right)$$

Where σ is the activation function (e.g., sigmoid, tanh, ReLU).

b. Output Layer Output (yk(t)):

$$y_k(t) = \Sigma_j w_{jk} \cdot z_j(t) + b_k$$

c. Training and Backpropagation:

During training, the weights and biases are adjusted to minimize a chosen loss function L. One common loss function for regression problems is the mean squared error:

$$L = \frac{1}{2N} \sum_{t=1}^{N} \left(y(t) - u(t)\right)^2 \quad (28)$$

The backpropagation algorithm is used to compute the gradients of the loss function with respect to the weights and biases. The weights and biases are then updated using gradient descent or other optimization algorithms. The weight update rule for the hidden layer weights *wij* is given by:

$$\Delta w_{ij} = -\eta \frac{\partial L}{\partial w_{ij}} \quad (29)$$

Where η is the learning rate.

The chain rule is applied to compute the partial derivatives in the backpropagation algorithm.

This is a simplified representation, and actual implementations may involve additional considerations, such as regularization techniques, different activation functions, and optimization strategies. The specific choice of these components depends on the characteristics of the control problem and the desired properties of the control algorithm [43-44].

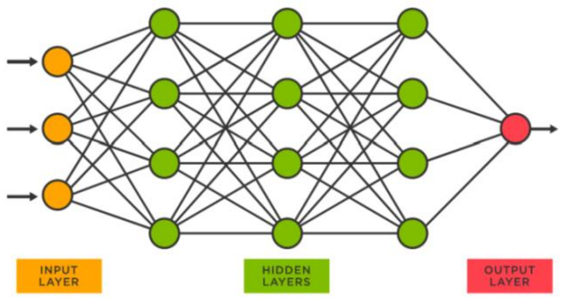

Figure 7. Design of a backpropagation network to provide a standard reference signal.

V. Policy Simulation Results and discussion

ANN-controlled Automatic Generation Control (AGC) frameworks for hydro-thermal power plants enhance grid management. Hydroelectric and thermal power plants are essential for electricity generation. Due to its dynamic nature, grid stability and frequency management demand innovative control approaches. In AGC frameworks for hydrothermal systems, artificial neural network (ANN) controllers have pros and cons.

Grid stability and performance depend on dynamic turbine time constants and changing power system demand. This study addresses these. Due to its flexibility and learning ability, ANN controllers can understand complex, nonlinear connections and make real-time control changes. In hydro-thermal power systems, artificial neural network controllers may increase grid stability and dependability. ANN controllers make advantage of neural networks' adaptive properties to optimise generation levels, reduce frequency deviations, and sustain grid functioning in dynamic circumstances. This study focuses on hydrothermal control using artificial neural networks (ANNs). Simulations and discussions compare ANN controller performance to conventional control methods. ANN controllers' grid stability performance is measured by frequency deviation, response time, and system stability. We also discuss practical challenges with ANN controllers in hydro-thermal power facilities. ANN controllers in AGC frameworks for hydro-thermal systems are investigated to enhance grid management. By advising energy operators and lawmakers, it aims to achieve efficient, reliable, and ecologically responsible grid operations. Further, the study describes how to model the hydro-thermal power system, create an AGC framework in MATLAB, and evaluate the ANN controller's performance by analysing simulation results to simulate the integration of an ANN controller for AGC in hydro-thermal systems.

A.Case: 1 Integration of ANN Controller for AGC in Hydro-Thermal Systems

In hydro-thermal systems with dynamic turbine time constants and changeable power system loading circumstances, a number of important discoveries are shown in the simulated outcomes of incorporating an Artificial Neural Network (ANN) controller for Automatic Generation Control (AGC) as shown in figure.8. To start, it's clear that the ANN controller is effective at controlling the system frequency even when the load is dynamic. Graphical representations of frequency deviation over time show that the controller reacts fast to changes in load, keeping the system frequency within the predefined limits. In addition, the system assesses how turbines with time constants that might change behave, simulating the dynamics of hydro and thermal generators. Visual representations of the turbine's reaction to changes in load illustrate how the ANN controller can adjust to different dynamics and maximise generating production appropriately. It is possible that the simulation will also show how well the controller maintains grid stability and dependability under various operating settings, providing further information about its resilience and stability. All things considered, the simulated results show that the ANN controller may improve the AGC performance in hydro-thermal systems, especially when dealing with dynamic turbine characteristics and changeable power system loading levels.

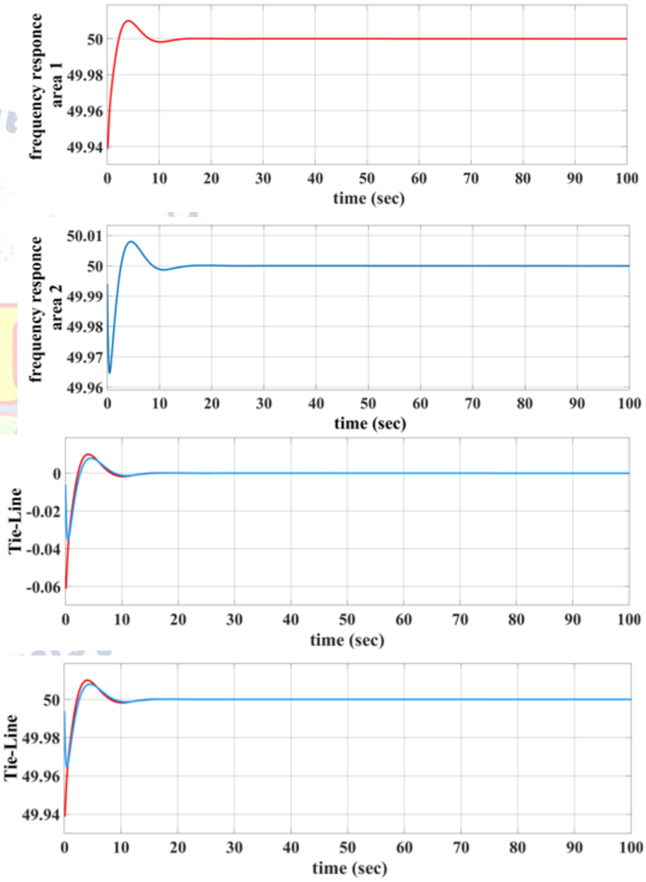

Figure.8 simulation results for Integration of ANN Controller for AGC in Hydro-Thermal Systems

B. Case: 2 Integration of integral Controller for AGC in Hydro-Thermal Systems

In hydro-thermal systems with dynamic turbine time constants and changeable power system loading circumstances, numerous important findings are made in the simulated outcomes of integrating an integral controller for Automatic Generation Control (AGC) as shown in figure.9. At the top of the display is the

integrated controller's performance in controlling the system frequency. The integrated controller's lightning-fast response to load fluctuations is shown graphically by the frequency deviation over time in the face of changing load circumstances. By doing so, it makes sure the system stays within reasonable bounds for the required frequency and reduces frequency deviations. In addition, the simulation analyses how wind turbines with variable time constants react to control commands from the integrated controller. Gain insights into the efficacy of the integrated controller's control operations by analysing charts illustrating turbine responsiveness to load variations. Contributing to grid stability and dependability, these findings showcase the controller's adaptability to dynamic turbine characteristics and its ability to optimise power output appropriately. All things considered, the simulation results show that the integral controller is good at improving the AGC performance in hydro-thermal systems, especially when dealing with dynamic turbine dynamics and changeable power system loading states.

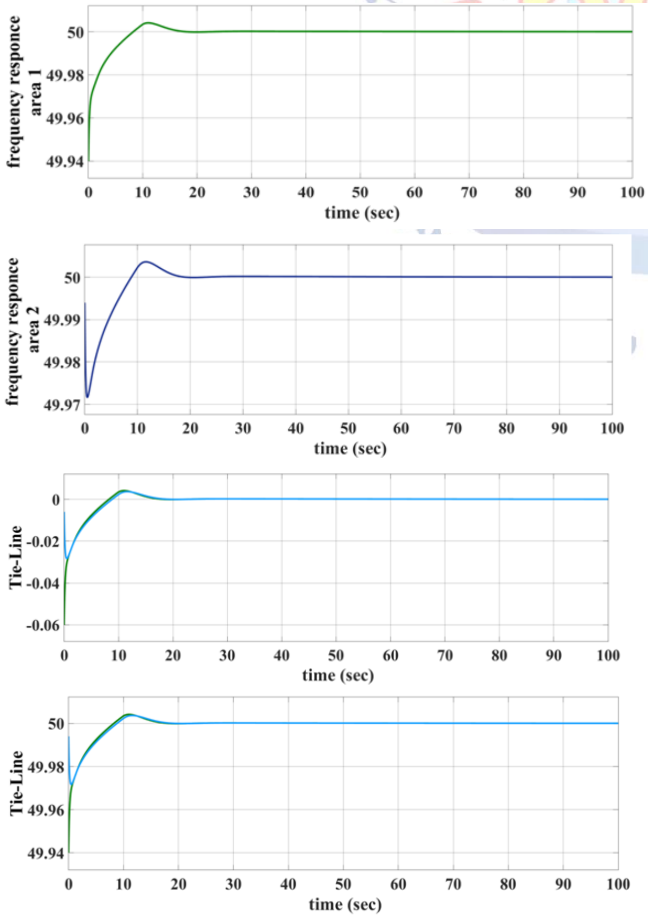

Figure.9 simulation results for Integration of integral Controller for AGC in Hydro-Thermal Systems

C. Integration of proportional integral Controller for AGC in Hydro-Thermal Systems

In hydro-thermal systems with dynamic turbine time constants and fluctuating power system loading circumstances, important insights are shown by the simulated results of incorporating a Proportional-Integral (PI) controller for Automatic Generation Control (AGC) as shown in figure.10. To start, it's clear that the PI controller is doing its job of controlling the system frequency. The PI controller reacts well to changes in load, as shown by graphs showing frequency deviation with time under different load situations. By keeping frequency variations to a minimum, it guarantees that the system will maintain the required frequency within reasonable limits. Turbines with variable time constants are also studied in the simulation in relation to the PI controller's control actions. The efficiency of the PI controller's operations may be better understood by analysing charts that show the turbine's reaction to variations in load. The findings demonstrate that the controller can adjust to the changing features of the turbines and maximise generating output in response, which helps keep the grid stable and reliable. When it comes to improving AGC performance in hydro-thermal systems, the PI controller really shines, according to the simulations. This is especially true when dealing with constantly changing turbine dynamics and power system loading situations.

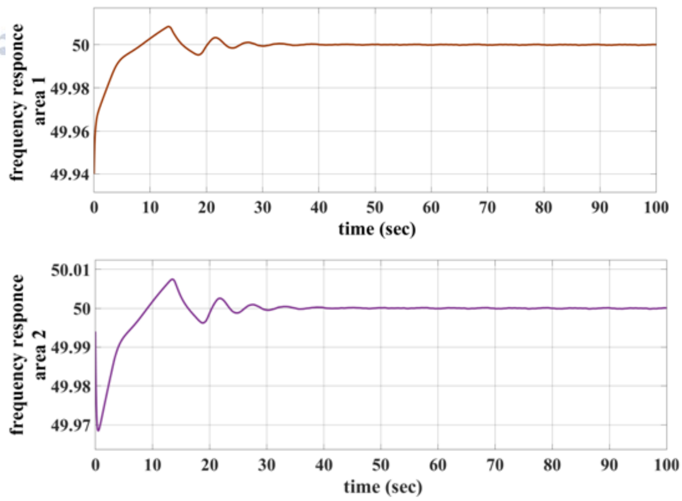

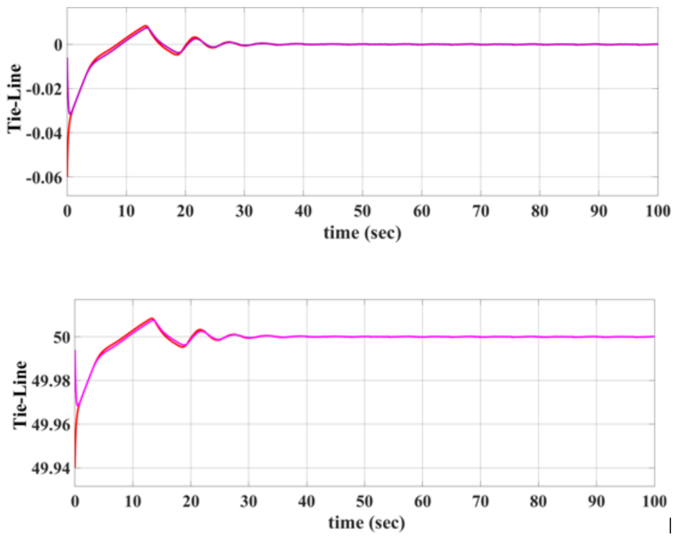

Fihure.10 simulation results for Integration of proportional integral Controller for AGC in Hydro-Thermal Systems

D. Case: 4 Simulation Results Comparison: ANN vs. Integral Controller and Integral vs. PI Controller

Simulated scenarios with highly dynamic load circumstances and changeable turbine dynamics show that the ANN controller works better than the integral controller as shown in figure.11. This is supported by the results of the comparison between the two controllers. Visualisations of time-varying frequency deviations show that the ANN controller keeps the target frequency within tighter limits and minimises frequency deviations, even when the load changes quickly. Because of its superior learning and adaptive capabilities, the ANN controller outperforms the integral controller in terms of accuracy and speed of reaction when regulating frequencies. When comparing the integral controller to the proportional-integral (PI) controller, it becomes clear that the integral controller performs better in certain cases. This is especially true when dealing with long-term disturbances or greatly fluctuating power system loads. An examination of the time-varying frequency deviation reveals that, in contrast to the PI controller, the integral controller recovers from disturbances more quickly and effectively, resulting in shorter settling periods and less oscillations. Because of this, the integral controller may improve the system's stability and resistance to shocks by strengthening corrective operations and constantly integrating error signals over time. By taking controller features and system dynamics into account, AGC techniques in hydro-thermal systems may be designed and implemented to achieve optimum performance under a wide range of operating situations.

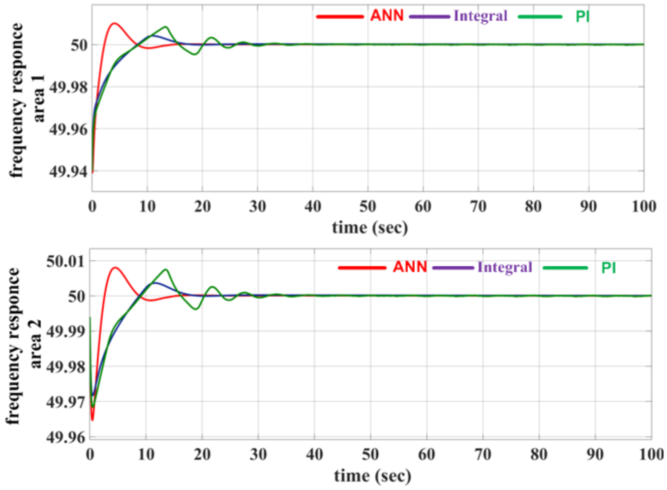

Figure.11 Simulation Results for Comparison of ANN vs. Integral Controller and Integral vs., PI Controller

VI. Conclusion

This paper presents the use of Artificial Neural Network (ANN) controllers for Automatic Generation Control (AGC) in hydro-thermal power systems. It demonstrates that ANN controllers can effectively manage non-linearities and uncertainties in hydro-thermal systems, ensuring optimal performance even under varying load conditions and transient disturbances. The ANN controller's robust learning mechanism allows for improved dynamic response, reduced settling time, and enhanced system stability. The integration of ANN for AGC also contributes to the reliability and efficiency of power systems by dynamically adjusting to changing conditions, minimizing the impact of load variations and turbine time constant fluctuations. This research underscores the potential of intelligent control strategies in modern power systems, paving the way for more resilient, efficient, and adaptive power management solutions. The adoption of ANN controllers in AGC operations represents a significant advancement in power system management, particularly for hydro-thermal systems with dynamic operational challenges.

Conflict of interest statement

Authors declare that they do not have any conflict of interest

REFERENCES

[1] S.M. Hietpas, M. Naden, "Automatic Voltage Regulator Using an AC Voltage–Voltage Converter," IEEE Trans. on Industry Applications, vol. 36, no. 1, pp. 33-38, 2000.

[2] E. Altıntas, O. Salor, U. Büyükdagl, "Correlation Between Multiple Electric Arc Furnace Operations and Unscheduled Power Flows in the Interconnection Lines at the Eastern Cross Border of ENTSO-E," IEEE Trans. on Industry Applications, vol. 52, no. 4, pp. 3508-3517, 2016.

[3] T.J. Roe, R.G. Baggs, C.R. Porcaro, "Computer Control of an Industrial Electrical System with In-Plant Generation," IEEE Trans. on Industry Applications, vol. IA-14, no. 5, pp. 387-396, 1978.

[4] K. G. Ravikumar, J. Bugshan, Scott Manson et. al, "Complete Power Management System for an Industrial Refinery," IEEE Trans. on Industry Applications, vol. 52, pp. 3565-3573, 2016.

[5] C. Concordia, L.K. Kirchmayer, "Tie-line Power and Frequency Control of Electric Power Systems," Power Appar. Syst., Trans. Am. Inst. Electr. Eng. Part III, vol. 72, no. 2, pp. 562-572, 1953.

[6] C. Concordia, L.K. Kirchmayer, "Tie-line Power and Frequency Control of Electric Power Systems- Part II," Power Appar. Syst., Trans. Am. Inst. Electr. Eng. Part III, vol. 73, no. 1, pp. 133-146, 1954.

[7] N. Cohn, "Some Aspects of Tie-line Bias Control on Interconnected Power Systems," IEEE Trans. Power Syst., vol. 75, no. 3, pp. 1415-1436, 1957.

[8] O.I. Elgerd, C.E. Fosha, "Optimum Megawatt Frequency Control of Multi-Area Electric Energy Systems," IEEE Trans. on Power Appar. Syst., vol. 4, pp. 556–563, 1970.

[9] C.E. Fosha, O.I. Elgerd, "The Megawatt-Frequency Control of Multiarea Electric Energy Systems," IEEE Trans. Power Appar. Sys., vol. PAS-89, no. 4, pp. 563-571, 1970.

[10] N. Pathak, I. Nasiruddin, T.S. Bhatti, "A More Realistic Model of Centralized Automatic Generation Control in Real-time Environment", Elect. Power Comp. Sys., vol. 43, no. 19, pp.1–9, 2015.

[11] I. Nasiruddin, P. Kumar, N. Hasan et. al, "Sub-optimal Automatic Generation Control of Interconnected Power System Using Output Vector Feedback Control Strategy," Elect. Power Comp. Syst., vol. 40, no. 9, pp. 977-994, 2012.

[12] J.J. Ibarra, M.I. Morales, W.J. Cabrera et.al, "AGC Parameter Determination for an Oil Facility Electric System," IEEE Trans. on Industry Applications, vol. 50, no. 4, pp. 2876-2882, 2014.

[13] J. Machowaski, J.W. Bialek, J.R. Bumby, "Power System Dynamics: Stability and Control," 5th edition, John Wiley & Sons Ltd., UK, 2008.

[14] A. Kumar, O.P. Malik, G.S. Hope, "Discrete variable structure controller for load frequency control of multiarea interconnected power systems," Gener. Transm. Distrib., IEE Proce. C, vol. 134, no. 3, p. 205, 1987.

[15] A. Kumar, O.P. Malik, G.S. Hope, "Variable-structure-system control applied to AGC of an interconnected power system," Gener. Transm. Distrib., IEE Proc. C, vol. 132, no. 1, pp. 23–29, 1985.

[16] E.V. Bohn and S.M. Miniesy, "Optimum Load-Frequency Sampled-Data Control with Randomly Varying System Disturbances," IEEE Trans. on Power Appar. Syst., vol. PAS-91, no. 5, pp.1916-1923, 1972.

[17] T. Hiyama, "Optimisation of discrete-type load-frequency regulators considering generation-rate constraints," Gener. Trans. Distrib., IEE Proc. C, vol. 129, no. 6. pp. 285–289, 1982.

[18] S. H. Hosseini, A. H. Etemadi, "Adaptive neuro-fuzzy inference system based automatic generation control," Electr. Power Syst. Res., vol. 78, no. 7, pp. 1230-1239, 2008.

[19] S.P. Ghoshal, "Optimizations of PID gains by particle swarm optimizations in fuzzy based automatic generation control," Elecrt. Power Syst. Res., vol. 72, no. 3, pp. 203-212, 2004.

[20] T.P. Imthias Ahamed, P.S. Nagendra Rao, P.S. Sastry, "A reinforcement learning approach to automatic generation control," Electr. Power Sysr. Res., vol. 63, no. 1, pp. 9-26, 2002.

[21] C.K. Shiva, V. Mukherjee, "Automatic generation control of multi-unit multi-area deregulated power system using a novel quasi-oppositional harmony search algorithm," IET Gener. Transm. Distrib., vol. 9, no. 15, pp. 2398–2408, 2015.

[22] R.K. Sahu, S. Panda, U. K. Rout, D. K. Sahoo, "Teaching learning based optimization algorithm for automatic generation control of power system using 2-DOF PID controller," Int. J. Electr. Power & Energy Syst., Elsevier, pp. 287-301, vol. 77, 2016.

[23] B. Mohanty, P. K. Hota, "Comparative performance analysis of fruit fly optimization algorithm for multi-area multisource automatic generation control under deregulated environment," IET Gener. Transm. Distrib., vol. 9, no. 14, pp. 1845-1855, 2015.

[24] H. Bevrani, F. Daneshfar, T. Hiyama, "A New Intelligent Agent-Based AGC Design with Real-Time Application," IEEE Trans. on Syst. Man Cybern., vol. 42, no. 6, pp. 994-1002, 2012.

[25] L.R. Chang-Chien, Y. S. Wu, J. S. Cheng, "Online estimation of system parameters for artificial intelligence applications to load frequency control," IET Gener. Transm. Distrib., vol. 5, no. 8, pp. 895–902, 2011.

[26] M. Vijay, D. Jena, "A Continuous-Discrete Mode of Optimal Control of AGC for Multi Area Hydrothermal System Using Genetic Algorithm", IEEE conf. on Comput. Communi. App. (ICCCA), pp.1-6, 2012.

[27] D.G. Ramey, J.W. Skooglund, "Detailed Hydro governor Representation for System Stability Studies," IEEE Trans. on Power Apprar. Syst., vol. PAS-89, no. 1, Jan 1970.

[28] J.M. Undrill, J.L. Woodward, "Nonlinear Hydro Governing Model and Improved Calculation for Determining Temporary Droop," IEEE Trans. on Power Apprar. Syst., vol. PAS-86, no.4, Apr 1967.

[29] S. Hagihara, H. Yokota, K. Goda et. al, "Stability of Hydraulic Turbine Generating Unit Controlled by P.I.D. Governor," IEEE Trans. on Power Apprar. Syst., vol. PAS-98, no. 6, Nov 1979.

[30] IEEE working group, "Hydraulic Turbine and Control Models for System Dynamic Studies," IEEE Trans. on Power Syst., vol. 7, no. 1, Feb 1992.

[31] L.N. Hannett, B. Fardanesh, "Field Tests to Validate Hydro Turbine-Governor Model Structure and Parameters," IEEE Trans. on Power Syst., vol. 9, no. 4, Nov 1994.

[32] K.S.S. Ramakrishna, P. Sharma, T.S. Bhatti, "Automatic generation control of interconnected power system with diverse sources of power generation," Int. J. of Engg. Sci. Tech., vol. 2, no. 5, pp. 51-65, 2010.

[33] Y. Sharma, L.C. Saikia, "Automatic generation control of a multi-area ST – Thermal power system using Grey Wolf Optimizer algorithm based classical controllers," Int. J. Electr. Power & Energy Syst., vol. 73, pp. 853-862, 2015.

[34][D. Puja, L.C. Saikia, S. Nidul, "Automatic generation control of multi area thermal system using Bat algorithm optimized PD–PID cascade controller," Int. J. Electr. Power & Energy Syst., vol. 68, pp. 364-372, 2015.

[35]N. Pathak, Ashu Verma, T.S. Bhatti, "Study the Effect of System Parameters on Controller Gains for Discrete AGC of Hydro-Thermal System," Annual IEEE India Conference (INDICON 2015), pp. 1-5, 17-20 Dec, 2015, New Delhi, India.

[36]J.J. Grainger, W.D. Stevenson, "Power System Analysis," McGraw Hill, New York, pp. 703-706, 1994.

[37]P. Kundur, "Power System Stability and Control," McGraw Hill, 8th edn., New York, pp. 422-424, 2009.

[38]F. Beaufays, Y. Abdel-Magid and B. Widrow, "Application of neural networks to load-frequency control in power systems," Neural Networks, vol. 7, Issue 1, pp. 183- 194, 1994.

[39]A. P. Birch. A.T. Sapeluk, C. S. Ozveren, "An enhanced neural network load frequency control technique," ControlConference Proceedings, no. 389, pp. 409- 415, 1994.

[40]D. K. Chaturvedi, P. S. Satsangi and P. K. Kalra, "Load frequency control: a generalised neural network approach," Electrical power engineering system, vol. 21, no. 6, pp. 405-415, 1999.

[41]A. Demiroren, N. S. Sengor, and H. Lale, "Automatic generation control by using ANN technique," Electric Power Components and Systems, vol. 29, no. 10, pp. 883-896, 2010.

[42]H. Shayeghi and H. Ali, "Automatic generation control of interconnected power system using ANN technique based on μ – synthesis," Journal of Electrical Engineering, vol. 55, no. 11, pp. 306–313, 2004.

[43]A. Demiroren, H. L. Zetnelgil and N. S. Sengor, "The application of ANN technique to for three-area power system," IEEE Porto Power Tech Conference, pp. 1–5, 2001.

[44]K. P. Wong, "Artificial intelligence and neural network: Applications in power systems," IEE 2nd International Conference on Advances in Power System Control, Operation And Management, no. December, pp. 37-46, 1993.